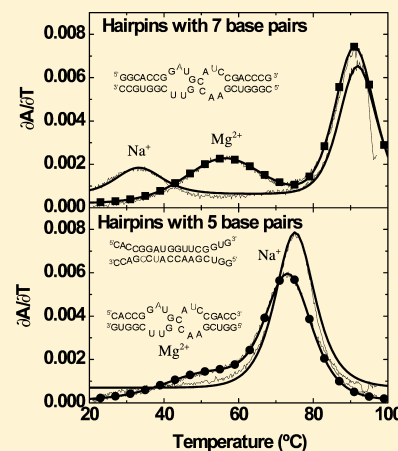


Effect of Helix Stability on the Formation of Loop–Loop Complexes

Preeti Sehdev,[†] Gordon Crews,[‡] and Ana Maria Soto^{*,†,‡}[†]Department of Chemistry, [‡]Molecular Biology, Biochemistry and Bioinformatics Program, Towson University, Towson, Maryland 21252, United States

ABSTRACT: Kissing loop complexes are loop–loop complexes where two RNA hairpins interact through their complementary loops. In this work, we have investigated the role of the helical stems on the ability of hairpins derived from the ColE1 plasmid to associate as kissing loop complexes in the presence and absence of divalent cations. Our results show that although kissing loop complexes form more readily in the presence of Mg^{2+} , they are able to form in the presence of 850 mM NaCl, as long as their stems contain at least six base-pairs. Formation of the Na^+ loop–loop complexes is facilitated by changing the sequence at the stem–loop interface to include less stable AU base pairs. We suggest that the conformation at the stem–loop interface is critical in the formation of kissing loop complexes and that in the absence of Mg^{2+} the conformation at the stem–loop interface is packed more loosely than with Mg^{2+} , to allow for a lower charge density. Consistent with this hypothesis, shortening the stems to five base pairs results in unfolding of the hairpins and formation of an extended duplex rather than a kissing loop complex because the short stems are not stable enough to tolerate the necessary conformation at the stem–loop interface to allow the formation of a kissing loop complex.



RNA plays a critical role in many cellular processes, including transcription, translation, splicing,¹ and gene regulation.² In order to accomplish its functions, RNA needs to fold into a precise three-dimensional structure.³ Hence, in order to fully understand the biological functions of RNA, it is important to understand the factors that govern the conformation of RNA.

“Kissing loop” complexes are loop–loop complexes where two RNA hairpins interact through their complementary loops⁴ (Figure 1). The formation of these complexes often promotes RNA–RNA recognition⁴ and is critical in a variety of processes,^{4,5} including the regulation of gene expression^{2,4} and virus packaging.⁶ Although in many cases the initial loop–loop complex progresses to a duplex, the formation of a full duplex is not always observed.⁴ Thus, the formation of kissing loop complexes per se is important for many biological functions. Furthermore, this motif is common in RNA tertiary folds⁷ and therefore can serve as a model for studying the factors affecting the conformation of RNA.

The structures of many kissing loop complexes^{6,8,9} show coaxial stacking of the stems of the individual hairpins, with the loops twisted in such a way that a continuous helix is formed. The formation of these complexes requires significant deformation of the loops on each hairpin, placing the bridging phosphates very close to each other⁹ and resulting in a significant build-up of charges.⁷ Hence, divalent ions such as Mg^{2+} are particularly important in the stability of kissing loop complexes,^{5,7} as is commonly observed in folded RNAs.^{10,11} However, some kissing loop complexes are able to form in the presence of moderate Na^+ concentrations,^{5,12,13} while others require the presence of divalent ions, such as Mg^{2+} , to form a

stable kissing loop complex.^{14,15} In particular, changing a few nucleotides in the loop sequence can sometimes lead to differences in the Mg^{2+} requirement.^{12,14,15} However, there is a need for studies investigating if small changes in the stems could have similar effects on the ability of hairpins to associate as kissing loop complexes and on the ionic requirements for their formation.

To better understand the role of the stems in the formation of kissing loop complexes, we have compared the formation of kissing loop complexes with identical loops but with small variations in the stems. We have studied kissing loop complexes with stems of varying length and also a complex in which a GC base pair near the loop is replaced with an AU base pair (Figure 1). Our results show that changing the sequence near the loop facilitates the formation of kissing loop complexes in the absence of Mg^{2+} . Furthermore, decreasing the stem length from seven to six base pairs does not affect the formation of loop–loop complexes. However, in the presence of 850 mM Na^+ , stems of five base pairs are not stable enough to maintain a kissing loop complex and result in the formation of a duplex. Our overall results suggest that the stem–loop interface is important in the formation of kissing loop complexes.

■ EXPERIMENTAL PROCEDURES

Materials. All RNA molecules were purchased from Integrated DNA Technologies (Coralville, Iowa) and purified using electrophoresis and electroelution. All experiments were

Received: April 14, 2012

Revised: September 30, 2012

Published: October 24, 2012

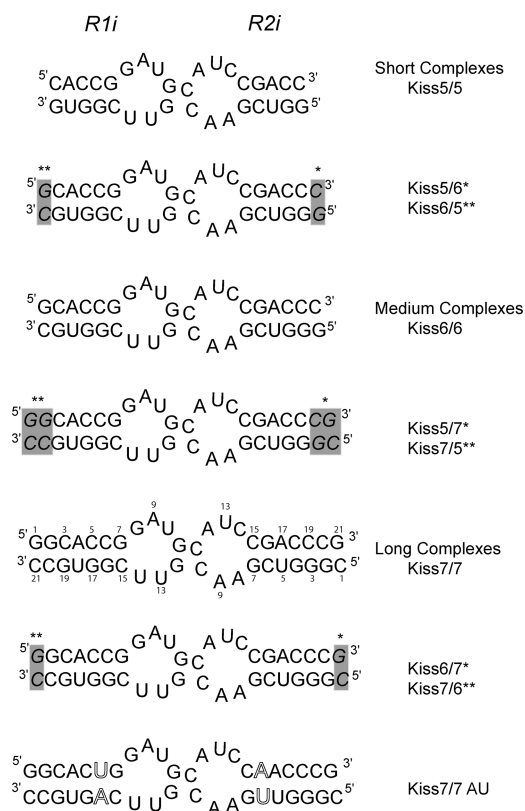


Figure 1. Molecules used in this work. * and ** refer to complexes with mixed stem sizes. In all nomenclature, the R1i hairpin is listed first. For example, Kiss 5/7 is made of an R1i hairpin with five base pairs in the stem and an R2i hairpin with seven base pairs in the stem.

conducted in 10 mM MOPS, pH 7 and various ionic strengths. The purified RNAs were extensively equilibrated in the appropriate solution before conducting experiments. All other chemicals were purchased from Sigma-Aldrich (St. Louis, Missouri) and used without further purification.

RNA and Ion Solutions. RNA concentrations were measured in water at 260 nm and 85 °C. At this high temperature (in water) the strands are unfolded and the extinction coefficients corresponding to the single strands can be used. The extinction coefficients used for each hairpin were as follows: R1i-5 = 164; R2i-5 = 161; R1i-6 = 180; R2i-6 = 178; R1i-7 = 197; R2i-7 = 195; R1i7-AU = 201; R2i7-AU = 199 $\text{mM}^{-1} \text{cm}^{-1}$. These coefficients were obtained from Integrated DNA Technologies (Coralville, Iowa) and can also be calculated from the sequence, as described previously.¹⁶ NaCl concentrations were calculated based on the NaCl weight, taking into account the purity of the reagent. The concentration of divalent ions solutions (Mg^{2+} , Ca^{2+} , Sr^{2+} , and Ba^{2+}) was measured by spectrophotometric titration with EDTA, as described previously.¹⁷ Briefly, 1000 μL of a ~ 1 mM divalent ion solution (MgCl_2 , CaCl_2 , SrCl_2 or BaCl_2) were placed in a semi-microcuvette and titrated with a 40 mM EDTA solution (which was previously calibrated using a MgCl_2 standard, purchased from Sigma). The end point of the titration was monitored by following the absorbance at 230 nm, which increases significantly when all the MgCl_2 has been titrated (because the free EDTA has a much larger extinction coefficient at 230 nm than the EDTA-metal ion complex).

UV Unfolding Experiments. UV melts (absorbance vs temperature profiles) were conducted in a thermoelectrically

controlled Cary 100 spectrophotometer equipped with a peltier. Cuvettes containing $\sim 4.6 \mu\text{M}$ (in total strands) solutions of the corresponding complex were heated at a rate of $0.2^\circ\text{C}/\text{min}$ and the absorbance at 260 and 280 nm were monitored. Each complex solution was prepared in the following way: 20–26 μM solutions of each hairpin in 10 mM MOPS, pH 7 were placed in a microcentrifuge tube, heated to 90°C for approximately 7 min and immediately cooled on ice for approximately 7 min. This procedure removes misfolded aggregates and facilitates the formation of hairpins.¹⁸ $\sim 6 \mu\text{M}$ solutions of each hairpin in 850 mM NaCl or 0.7 mM MgCl_2 were prepared by mixing appropriate amounts of the refolded hairpins, 10 mM MOPS buffer and NaCl or MgCl_2 stocks. Finally, equimolar amounts of the corresponding hairpins were placed in a semi-microcuvette and the appropriate amounts of 10 mM MOPS buffer and NaCl or MgCl_2 stocks were added to obtain 1500 μL of solutions with final concentrations of $\sim 2.3 \mu\text{M}$ of each hairpin, 850 mM NaCl or 0.7 mM MgCl_2 . Control experiments with the individual hairpins were prepared in the same way except that only one of the hairpins was added to the cuvette. For the majority of the complexes, the resulting unfolding profiles have two transitions, which are difficult to analyze using the direct unfolding profiles. Hence, the enthalpy (ΔH) of unfolding and the unfolding temperature (T_m) of each transition were obtained by analyzing the first derivatives of the resulting UV melts. ΔH was obtained by applying the following equations to the first derivatives of the unfolding profiles, as described previously:¹⁹ $\Delta H = (B)/((1/T_1) - (1/T_2))$ or $\Delta H = (B')/((1/T_m) - (1/T_2))$, where B and B' are constants corresponding to the molecularity of the transition (for monomolecular transitions, $B = -7$ and $B' = -3.5$; for bimolecular transitions, $B = -10.14$ and $B' = -4.38$), T_m is temperature (in K) at which the change in absorbance (dA/dT) is maximum, and T_1 and T_2 are the lower (T_1) and upper (T_2) temperatures (in K) at which the change in absorbance is equal to half of the maximum. Unfolding enthalpies and T_m 's were also obtained using the program Global Melt Fit, developed by D. E. Draper,^{20,21} but the enthalpies for the first transition obtained with this program were multiplied by 1.449 ($10.14 \div 7$) because the fitting was done assuming a monomolecular transition. Both methods give the same enthalpies and T_m 's, within the error. Folding entropies (ΔS_{fold}) for kissing loop complexes were calculated based on the T_m (in Kelvin), folding enthalpies (ΔH_{fold}), total strand concentrations (C_T , in molar units) and the gas constant (R), using the following equation for bimolecular transitions: $1/T_m = R/\Delta H_{\text{fold}} \ln(C_T/4) + (\Delta S_{\text{fold}}/\Delta H_{\text{fold}})$, as described previously.¹⁹ Unfolding experiments, starting from the preparation of new stocks were conducted at least twice.

UV Titrations. The formation of the loop–loop complexes was monitored by following the decrease in absorbance at 260 nm upon the addition of increasing concentrations of Mg^{2+} or Na^+ , using a Cary 100 spectrophotometer. For each experiment, a $\sim 7 \mu\text{M}$ solution of each hairpin in 10 mM MOPS pH 7 was placed in a microcentrifuge tube. The tube was heated to 90°C for 7 min and immediately cooled on ice for another 7 min. Equimolar amounts of hairpins with complementary loops (see Figure 1) were mixed in a semimicro quartz cuvette to yield a final volume of 800 μL . The solutions were then titrated using 8–100 μL aliquots of a ~ 2 M NaCl stock solution or 1–3 μL aliquots of a ~ 25 mM MgCl_2 stock solution. The solutions were equilibrated for 20–60 min after each injection (until the signal was stable), and the absorbances at 260 and 350 nm were

recorded. The absorbance at 350 nm was subtracted from the absorbance at 260 nm to correct for scattering arising from chemically inert particulate contaminants. The resulting absorbance was further corrected by multiplying it by the dilution factor. The majority of the experiments were conducted using complex concentrations of exactly 3.5 μM (formed by mixing 3.5 μM of each hairpin). Experiments in which the concentration was slightly below or above 3.5 μM were normalized by dividing the absorbance by the measured concentration of complex and multiplying it by 3.5. Normalization is necessary because all molecules have the exact same loops so a direct comparison of the loop–loop complexes requires equal concentration of the loops.

The titration curves of the different complexes start at different absorbance values because the size of the stems in each complex varies (thus, a 3.5 μM solution of a complex with longer stems will absorb more light than a 3.5 μM solution of a complex with shorter stems). To better compare the titrations, the data presented are displaced (by adding or subtracting the appropriate number) such that all curves start at an absorbance of 1. All titrations, starting from the preparation of new stocks, were conducted at least two times.

Circular Dichroism Experiments. CD spectra were collected using a Jasco J815 spectropolarimeter. Solutions were prepared in the same way as for the UV melts except that more solution was made (the final volume was 2050 μL). The resulting complexes were incubated at room temperature for at least 2 h before recording the CD spectra. The spectra shown in Figure 4 represent the average of at least three consecutive runs; all spectra were corrected by subtracting the spectra of the buffer (collected in the same cuvette). The molar ellipticity was calculated as follows: the corrected CD signal (ellipticity) was divided by the total concentration of strands (in molar units) and was multiplied by 100^{22,23} to yield units of degrees $\times \text{cm}^2 \times \text{dmol}^{-1}$. CD experiments, starting from the preparation of new stocks, were conducted at least two times.

RESULTS

Molecules. The kissing loop complexes used for these studies are derived from the ColE1 bacterial plasmid. We used the modified ColE1 system, in which the loop sequences are inverted, compared to the wild type, to improve stability.^{9,18,24} Each kissing loop complex is composed of two hairpins with complementary loops, designated R1i and R2i. In order to determine whether the length of the helical stem affects the formation of loop–loop complexes, we compared a variety of complexes containing the exact same loops with varying stem lengths. We classified these complexes as short (with five base pairs in each stem or combinations of hairpins with six and five base pairs in the stems: Kiss5/5, Kiss5/6, Kiss6/5), medium (with six base pairs in each stem or combinations of hairpins with seven and five base pairs in the stems, Kiss6/6, Kiss5/7 and Kiss7/5), and long (with seven base pairs in the stems or combinations of six and seven base pairs in the stems: Kiss7/7, Kiss6/7 and Kiss7/6). In addition, we also studied a long complex in which a GC base pair near the stem–loop interface was replaced with an AU base pair (Kiss7/7-AU). In all cases, the number immediately following the word “Kiss” refers to the R1i hairpin and the second number refers to the R2i hairpin. All molecules are shown in Figure 1.

UV Titrations. The formation of each loop–loop complex was monitored by performing UV titrations at room temperature. As increasing concentrations of NaCl or MgCl_2 are added

to a cuvette containing a mixture of the corresponding R1i and R2i hairpins, the absorbance at 260 nm decreases. The decrease corresponds to the formation of base pairs and stacking of bases upon formation of each kissing loop complex, rendering the bases less exposed to the solvent. Our results show that all hairpin mixtures are able to form some sort of complex, presumably a kissing loop complex, in the presence of Mg^{2+} , as observed by the similar decrease in absorbance upon addition of MgCl_2 (Figure 2a). However, in the presence of NaCl

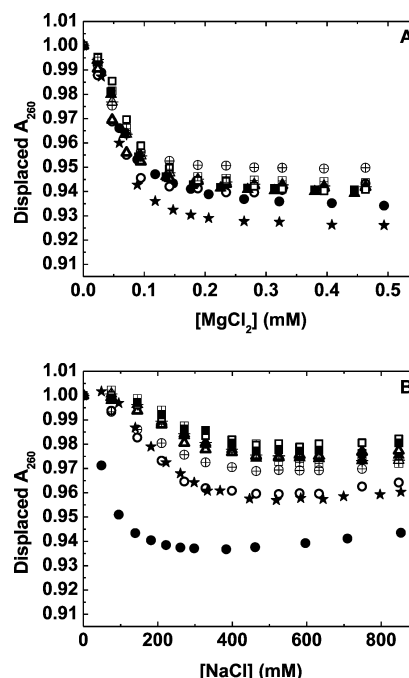


Figure 2. UV titrations of kissing complexes with MgCl_2 (Panel A) or NaCl (Panel B). Complexes are represented by circles (short complexes), triangles (medium complexes) or squares (long complexes): Kiss 5 (●), Kiss 5/6 (○), Kiss 6/5 (⊕), Kiss 6 (▲), Kiss 5/7 (△), Kiss 7/5 (open triangle with cross), Kiss 7 (■), Kiss 6/7 (□), Kiss 7/6 (⊞), AU-kiss (★). All experiments were conducted in 10 mM MOPS pH 7, using a total strand concentration of 7 μM (or normalized to this concentration). To facilitate visual comparison, the absorbance of each titration was displaced by adding or subtracting the corresponding value such that each titration starts at 1 absorbance units.

(Figure 2b) only the shortest complex (Kiss 5/5) decreases in absorbance to a similar extent as in the presence of MgCl_2 . The other hairpins are able to form some kind of complex but seem to require much higher NaCl concentrations, and their absorbance does not decrease as much as in the presence of Mg^{2+} . The short complexes containing at least one of the hairpins with five base-pair stems (Kiss5/6 and Kiss6/5) display intermediate decreases in absorbance suggesting that the presence of at least one short hairpin facilitates the formation of some kind of complex at 850 mM NaCl. Replacing a GC base pair for an AU base pair in the longest complex seems to facilitate the formation of some kind of complex (as observed by the larger hypochromicity of Kiss7/7-AU compared to Kiss7/7).

UV Melts and Circular Dichroism Experiments. The conformation and stability of the individual hairpins and of each loop–loop complex were monitored using circular dichroism and UV thermal denaturation experiments (UV melts). Specific

details about each system are described below but, in general, the hairpins unfold in single transitions while the kissing loop complexes (except Kiss5/5) unfold in two or three transitions. The complexes that combine hairpins with different stem lengths (Kiss 5/6, 6/5, 5/7, 7/5, 6/7 and 7/6) show three transitions, while the complexes that contain hairpins with the same stem length (Kiss 6/6, 7/7 and AU) show two transitions. The first transition corresponds to the unfolding of the complex formed between the hairpins, presumably a kissing loop complex, the second transition is the unfolding of the shorter hairpin (or the simultaneous unfolding of two hairpins of the same length for the 5/5, 6/6, 7/7 and AU complexes), and the third transition is the unfolding of the longer hairpin.

Individual Hairpins. Table 1 summarizes the unfolding of the individual hairpins. All hairpins unfold in single transitions,

Table 1. Unfolding Profiles of Individual Hairpins in NaCl and MgCl₂^a

hairpin	nearest neighbors	850 mM NaCl		0.7 mM MgCl ₂	
	ΔH kcal/mol	ΔH kcal/mol	T_m °C	ΔH kcal/mol	T_m °C
R1i-5	42.3	48	74.4	43	76.5
R2i-5	44.3	48	72.2	49	73.3
R1i-6	57.1	64	85	59	84.8
R2i-6	57.7	66	84.5	65	84.7
R1i-7	70.5	72	93	75	90.9
R2i-7	68.3	69	91.8	70	91.5
R1i7-AU	67.4	72	85	73	83.7
R2i7-AU	62.5	69	83	65	83.4

^aAll experiments were conducted using a total strand concentration of 2.3 μ M in 10 mM MOPS pH 7 and 850 mM NaCl or 0.7 mM MgCl₂, as indicated. Expected enthalpies were calculated using the nearest neighbor parameters from ref 25.

with van't Hoff enthalpies consistent with the number of base pairs in their stems (as estimated by the nearest neighbor parameters²⁵).

Kiss7/7. As expected, Kiss7/7, our longest complex, unfolds in two transitions both in the presence of 0.7 mM Mg²⁺ or 850 mM Na⁺ (Figure 3A,B). The first transition corresponds to the kissing loop complex because it unfolds with enthalpies that are reasonable for seven base-pair kissing loop complexes: 48 kcal/mol (in Mg²⁺) and 61 kcal/mol (in Na⁺). The second transition corresponds to the simultaneous unfolding of the individual hairpins as it unfolds with very similar profiles as the individual hairpins. The circular dichroism spectra (Figure 6G) of Kiss7/7 in Na⁺ and Mg²⁺ are very similar, suggesting that both ions promote the formation of loop–loop complexes, albeit with some differences.

Kiss7/6 and Kiss 6/7. In the presence of 850 mM NaCl or 0.7 mM MgCl₂, Kiss6/7 and Kiss7/6 unfold in three transitions (Figure 3C–F), with parameters that suggest the formation of kissing loop complexes (Tables 2 and 3). At a first glance, the second and third transitions appear to be one transition because the T_m 's of the hairpins with six base pairs are close to the T_m 's of the hairpins with seven base pairs. However, the sum of the individual hairpin transitions superimposes the second/third transitions of Kiss6/7 and Kiss7/6, strongly suggesting that the second/third transitions correspond to the unfolding of the individual hairpins. The circular dichroism spectra of Kiss6/7 and Kiss7/6 (Figure 6H,I) suggest that both kissing loop

complexes are able to form in the presence of Na⁺ or Mg²⁺, as indicated by the similarity of the spectra in 850 mM NaCl and 0.7 mM MgCl₂.

Kiss6/6. Kiss6/6 unfolds in two transitions (Figure 4A,B), with parameters that suggest the formation of kissing loop complexes in the presence of 850 mM NaCl or 0.7 mM MgCl₂. Furthermore, its CD spectra with Na⁺ and Mg²⁺ are similar, suggesting the formation of kissing loop complexes with both kinds of ions (Figure 6D).

Kiss5/7 and Kiss7/5. In the presence of 0.7 mM MgCl₂, Kiss5/7 and Kiss7/5 unfold in three transitions (Figure 4C,E) with enthalpies that are consistent with the formation of a kissing loop complex (Table 2). However, several irregularities are observed in the presence of 850 mM NaCl (Figure 4D,F). Each complex unfolds in four transitions with the last two transitions representing the sum of the individual hairpins, although with some deviations (for instance the sum of the hairpins is not fully superimposable in Kiss7/5). The presence of two initial transitions indicates the presence of competing equilibria, perhaps representing two alternative structures. In Kiss5/7, none of these structures is consistent with a kissing loop complex because the enthalpies of unfolding are very large (100–140 kcal/mol). In the case of Kiss7/5 one of the alternative complexes may be a kissing loop complex because the enthalpy of the first transition is 55 kcal/mol, but the enthalpy of the second transition is too large (210 kcal/mol) to represent a kissing loop complex. The circular dichroism spectra of the sodium complexes (Figure 5E,F) are similar to the spectra of the Mg²⁺ complexes, although Kiss5/7 shows somewhat significant deviations, consistent with the irregularities observed in the unfolding patterns.

Kiss5/6 and Kiss6/5. In the presence of 0.7 mM MgCl₂, Kiss5/6 and Kiss6/5 unfold in three transitions (Figure 5C,E), with enthalpies characteristic of the formation of a kissing loop complex (Table 2). However, in the presence of 850 mM NaCl (Figure 5D,F), Kiss5/6 and Kiss6/5 appear to form alternative complexes rather than kissing loop complexes. Both complexes unfold in four transitions, with the last two transitions corresponding to the unfolding of the individual hairpins but displaying deviations (the sums of the individual hairpins are not fully superimposable). One of the first two transitions in Kiss6/5 has an enthalpy that is too large to represent a kissing loop complex (196 kcal/mol) while the second transition (51 kcal/mol) may represent a kissing complex. Kiss5/6 has an enthalpy that could represent a kissing complex (54 kcal/mol), but it also has a small additional peak that suggests the presence of a competing equilibrium. In addition, it is worth noting that the first half of the transition does not fit very well and seems to be steeper than the fitted curve. We had initially attributed this deviation to an instrumental error, but it is highly reproducible and it appears in all the repetitions we have conducted. Furthermore, the circular dichroism spectra of the Na⁺ complexes are different than the spectra of the Mg²⁺ complexes, suggesting again the presence of alternative complexes. These results also suggest that the intermediate decreases in absorbance observed in the Na⁺ titrations of Kiss5/6 and Kiss6/5 may arise from the partial formation of extended duplexes and that these structures may exist in an equilibrium between duplexes and loop–loop complexes.

Kiss5/5. In the presence of 0.7 mM MgCl₂, Kiss5/5 unfolds in two transitions (Figure 5A). The enthalpy of the first transition (36 kcal/mol) suggests the formation of a kissing loop complex, while the second transition corresponds to the

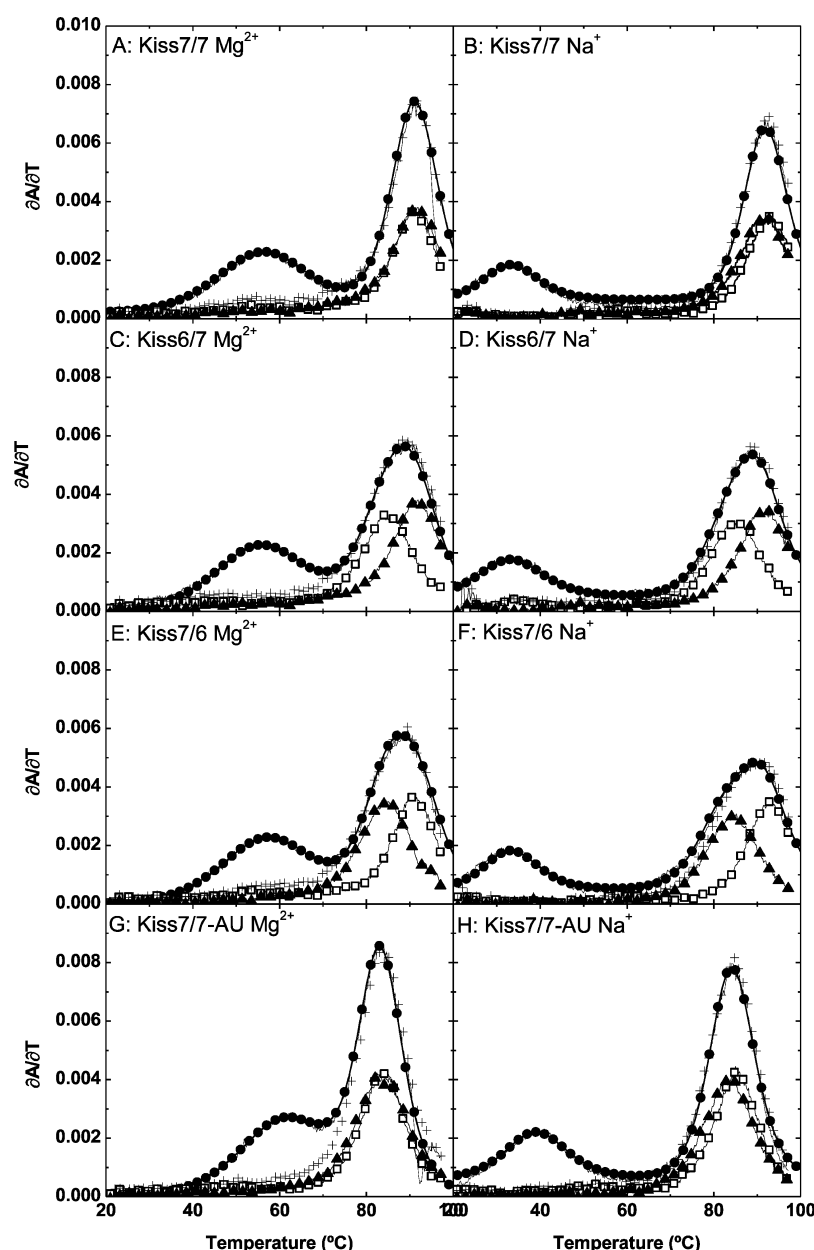


Figure 3. Unfolding of long kissing loop complexes in 0.7 mM MgCl_2 (left panels) or 850 mM NaCl (right panels). A and B: Kiss7/7; C and D: Kiss6/7; E and F: Kiss7/6; G and H: Kiss7/7-AU. In each panel, the complexes are represented with filled circles, the R1i hairpins are represented by open squares, the R2i hairpin is filled triangles and the sum of the hairpins are lines with plus (+) signs. All experiments were conducted in 10 mM MOPS pH 7, using a total strand concentration of 2.3 μM (hairpins) or 4.6 μM (complexes). The traces shown represent the first derivative of the absorbance vs temperature profiles collected at 260 nm.

unfolding of the individual hairpins. The sum of the individual hairpins does not fully superimpose the second transition, but this is because in this case the kissing loop complex and the individual hairpins transitions partially overlap. However, significant deviations are observed in the presence of 850 mM NaCl . A single transition is observed in the presence of NaCl (Figure 5B), indicating that the short complex and the stems unfold simultaneously. Furthermore, the enthalpy of this complex is about 116 kcal/mol (it unfolds in a non-two-state transition that can be deconvoluted into two transitions with enthalpies of 116 and 50 kcal/mol). We hypothesize that this short complex forms a kissing loop complex, but it immediately progresses to a duplex, resulting in the formation of a duplex with mismatches, which unfolds in a single transition. This

hypothesis is supported by the expected enthalpy of unfolding of a duplex with 11 base pairs and 2 wobble GU base pairs (predicted to be between 107 and 135 kcal/mol for a duplex of 11–13 base pairs, based on the nearest neighbor parameters²⁵). The fact that the shortest complex forms a duplex rather than a kissing loop complex in the presence of NaCl suggests that the five base pairs of these stems are unable to tolerate the conformational changes that may occur upon formation of the Na^+ loop–loop complex. The circular dichroism spectra (Figure 6A) further suggest the formation of a duplex. Kiss5/5 exhibits significantly different spectra in the presence of NaCl and MgCl_2 , with the Na^+ complex strikingly similar to the sum of the individual hairpins. The similarity between the Na^+ complex spectrum and the spectra of the individual

Table 2. Unfolding Profiles of Kissing Complexes in MgCl_2^a

complex	Transition 1		Transition 2		Transition 3	
	ΔH_1^* kcal/mol	T_{m1} °C	ΔH_2 kcal/mol	T_{m2} °C	ΔH_3 kcal/mol	T_{m3} °C
Kiss5/5	36	53	58	73.5	N/A	N/A
Kiss56	44	57	50	77.2	60	85.7
Kiss65	44	57	60	73	67	85
Kiss6/6	44	58	65	85	N/A	N/A
Kiss57	46	55	50	77	75	91.5
Kiss75	44	58	63	73.3	69	91.7
Kiss67	42	56.5	61	85	67	91.3
Kiss76	46	57.9	65	84.9	70	91.7
Kiss7/7	48	57	73	91.3	N/A	N/A
Kiss7/7-AU	45	62.1	75	83.3	N/A	N/A

^aAll experiments were conducted in 10 mM MOPS pH 7, 0.7 mM MgCl_2 , using a total strand concentration of 4.6 μM .

Table 3. Unfolding Profiles of Kissing Complexes in NaCl^a

complex	Transition 1		Transition 2		Transition 3	
	ΔH_1^* kcal/mol	T_{m1} °C	ΔH_2 kcal/mol	T_{m2} °C	ΔH_3 kcal/mol	T_{m3} °C
Kiss5/5	116	75.3	50	75.3	N/A	N/A
Kiss56	54	31.5	47	75.5	61	83.5
Kiss65	51/196	45/39	47	74.5	72	85.5
Kiss6/6	65	33.5	67	84.5	N/A	N/A
Kiss57	100/140	36.5/ 50.5	50	75	75	91.5
Kiss75	55/210	32/40.5	48	73.5	75	93
Kiss67	55	33.5	60	84	70	90.5
Kiss76	62	33.5	60	82.5	70	91.5
Kiss7/7	61	33.3	77	92	N/A	N/A
Kiss7/7-AU	64	39.3	74	84.3	N/A	N/A

^aAll experiments were conducted in 10 mM MOPS pH 7, 850 mM NaCl, using a total strand concentration of 4.6 μM .

hairpins strongly suggests that the short complex forms a duplex, which acquires the expected A-conformation that also characterizes the stems of the individual hairpins.

Kiss7/7-AU. Kiss7/7-AU unfolds in two transitions in the presence of 850 mM NaCl and 0.7 mM MgCl_2 (Figure 3G,H). In both cases, the first transition corresponds to the unfolding of the kissing loop complex, with enthalpies of 45–64 kcal/mol (Tables 2 and 3), while the second transition corresponds to the simultaneous unfolding of the individual hairpins (as it superimposes the sum of the individual hairpins). Furthermore, the circular dichroism spectra of the Na^+ and Mg^{2+} complexes are very similar, suggesting the formation of loop–loop complexes with both ions. However, as shown in Table 4, Kiss7/7-AU is more stable than Kiss7/7 under all conditions indicating that replacement of a GC base pair with an AU base pair at the stem–loop interface favors the formation of kissing loop complexes.

Ionic Environment Effects. To determine if the apparent differences between the Na^+ and Mg^{2+} complexes arise from the presence of specific Mg^{2+} sites, we analyzed the formation of Kiss7/6 using Ca^{2+} , Sr^{2+} , Ba^{2+} and larger concentrations of Na^+ (Figure 7A,B and Table 5). Although all divalent ions form kissing loop complexes, Sr^{2+} and Ba^{2+} form less stable complexes and their absorbance does not decrease as much as in the presence of Mg^{2+} or Ca^{2+} . Increasing the

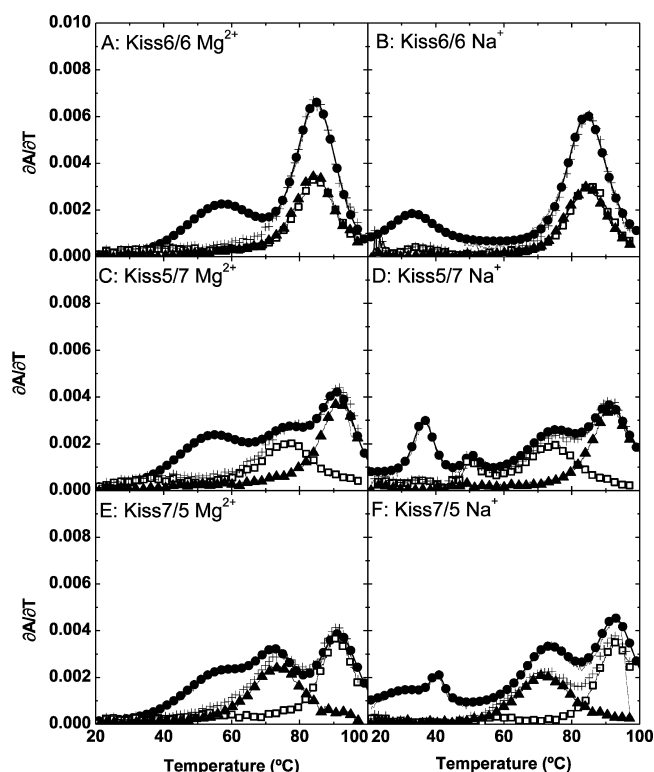


Figure 4. Unfolding of medium kissing loop complexes in 0.7 mM MgCl_2 (left panels) or 850 mM NaCl (right panels). A and B: Kiss6/6; C and D: Kiss5/7; E and F: Kiss7/5. In each panel, the complexes are represented with filled circles, the R1i hairpins are represented by open squares, the R2i hairpin are filled triangles and the sum of the hairpins are lines with plus (+) signs. All experiments were conducted in 10 mM MOPS pH 7, using a total strand concentration of 2.3 μM (hairpins) or 4.6 μM (complexes). The traces shown represent the first derivative of the absorbance vs temperature profiles collected at 260 nm.

concentration of NaCl stabilizes the kissing loop complex but does not promote the same decrease in absorbance as Mg^{2+} or Ca^{2+} ; in fact, it produces unusual titration profiles. Finally, to determine if Kiss5/5 simply requires higher Na^+ concentrations to form a kissing loop complex, we have monitored the formation of Kiss5/5 with larger amounts of Na^+ (Figure 7C). Increasing the concentration of NaCl up to 2.7 M does not promote the formation of a kissing loop complex in Kiss5/5. Kiss5/5 forms a duplex rather than a kissing loop complex even at very high NaCl.

The combined results indicate that the presence of small divalent ions (Mg^{2+} or Ca^{2+}) or AU base pairs at the stem–loop interface facilitates the formation of kissing loop complexes, while the presence of short hairpins (R1i5 or R2i5) promotes the formation of extended duplexes when only NaCl is present.

DISCUSSION

Kissing Loop Complex Formation. The titration experiments described above monitor the formation of the loop–loop complexes by the decrease in absorbance that occurs upon interaction of the loops. This decrease corresponds to the formation of base pairs and stacking interactions within the loops, effectively shielding the bases from the solvent and decreasing their molar absorptivity. However, it is possible that the decrease in absorption reflects self-association of the

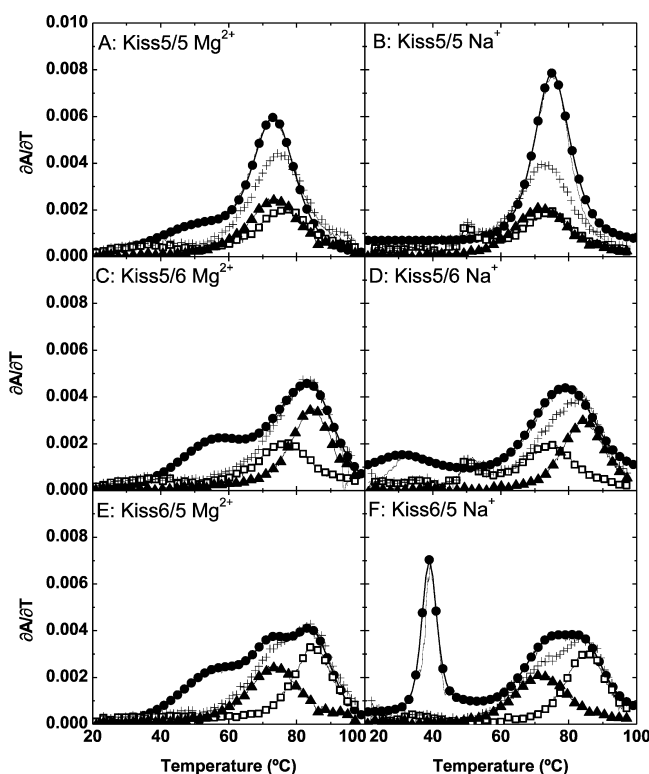


Figure 5. Unfolding of short kissing loop complexes in 0.7 mM MgCl_2 (left panels) or 850 mM NaCl (right panels). A and B: Kiss5/5; C and D: Kiss5/6; E and F: Kiss6/5. In each panel, the complexes are represented with filled circles, the R1i hairpins are represented by open squares, the R2i hairpin is filled triangles and the sum of the hairpins are lines with plus (+) signs. All experiments were conducted in 10 mM MOPS pH 7, using a total strand concentration of 2.3 μM (hairpins) or 4.6 μM (complexes). The traces shown represent the first derivative of the absorbance vs temperature profiles collected at 260 nm.

hairpins or the formation of a duplex rather than a kissing complex.

Discarding Self-Association of Hairpins. Our UV unfolding experiments suggest that the R1i hairpins have a small tendency to self-associate, while the R2i hairpins do not appear to self-associate. The tendency of the R1i hairpins to self-associate can be observed in some UV unfolding experiments as a small sharp peak at around 50 °C (Figure 5) that appears to occur only when the kissing loop complex or extended duplex does not form (either after the complex has unfolded or when only the R1i hairpins are present (individual hairpins melts)). This suggests that the kissing loop complex or extended duplex are more stable (at low temperature) than the R1i dimers. R1i may self-associate more readily than R2i due to the sequence of its loop, which could form three base pairs (1 AU and 2 GU). However, the tendency to self-associate is small, indicating that the R1i hairpin is more stable than the R1i dimers, especially when the R2i hairpins are present and the formation of a more stable complex between the R1i and R2i hairpins is possible.

Extended Duplex vs Kissing Loop Complexes. Since the hairpins have complementary loops, they could form extended duplexes rather than kissing loop complexes. Depending on the length, such duplexes would contain four to six mismatches and two G-U wobble base pairs due to the noncomplementary hairpin stems. Although we cannot

distinguish the imperfect duplex from the kissing loop complex based on the UV absorption data or gel retardation experiments (as both complexes are of about the same size), we should be able to distinguish them based on their unfolding profiles (Figures 3 and 4). An extended duplex is expected to unfold in a single, non-two-state transition (due to the presence of mismatches), while a kissing loop complex should show the dissociation of the kissing loop complex followed by the unfolding of the hairpins. Although the presence of more than one transition does not guarantee the presence of kissing loop complexes (as discussed below), the unfolding pattern combined with the ΔH values can suggest the presence of kissing loop complexes. Experimental ΔH values of ~ 48 kcal/mol have been observed in the unfolding of ColE1 kissing loop complexes in 5 mM MgCl_2 ,¹⁸ and values of 35–75 kcal/mol have been observed in the unfolding of HIV dimerization initiation signal (DIS) type kissing complexes in 1 M NaCl .²⁶ Although the HIV DIS kissing complexes used in ref 26 contain nine nucleotide loops, only six nucleotides are complementary, so its unfolding enthalpy should be comparable to our ColE1 system, which contains seven base pairs in the loops. ΔH values of ~ 50 kcal/mol are also consistent with the NMR structure of the ColE1 complex,⁹ which shows that although all possible base pairs are formed (seven base-pairs = six base-pair stacks), there are significant deviations for the A-form geometry. Thus, our experimental values indicate that all hairpins form kissing loop complexes in the presence of 0.7 mM MgCl_2 and that the complexes containing hairpins with six or more base pairs stems also form complexes in the presence of 850 mM NaCl . In the presence of 850 mM Na^+ , the complexes containing at least one hairpin with five base pair stems display unfolding profiles that suggest the presence of a different kind of complex. Some of these complexes display multiple transitions because after unfolding of the alternative complex, the temperature is relatively low so the individual hairpins are still stable enough to refold. This refolding of the hairpins upon unfolding of a duplex has been observed before,²⁷ and it explains why the majority of complexes show transitions corresponding to the unfolding of the hairpins at high temperature.

Kissing Loops Structure. The NMR or crystal structures of several kissing loop complexes have been solved.^{6,8,9,28} In all cases, there is continuous stacking of all the bases starting in one of the stems, followed by the bases in the loop–loop region and ending with the bases of the second stem. A model based on the coordinates of the ColE1 kissing complex, the sequence used in this work (Protein Data Bank file 2BJ2⁹), is shown in Figure 8 (prepared using SwissPdbViewer²⁹). The overall structure is bent toward the major groove and two bridging phosphates (the phosphates of the purines closing the loops in each hairpin, G8 and A8 in Figure 1, which are shown as space filled nucleotides in Figure 8) cross the major groove, allowing continuous stacking of all the bases by bridging the three helices (the two stems and the loop helices). The bending of the structure shortens the distance that the bridging phosphates (shown as yellow spheres in Figure 8) need to cross because it narrows the major groove,^{9,18} facilitating the formation of the complex. The bridging phosphates as well as other phosphates around the loop–stem junction are very close together (for instance, the reported distance between the bridging phosphates is 5.29 Å, which is 0.61 Å closer than the typical distance between sequential phosphates),⁹ creating a region of very high charge density. This high charge density explains the requirement of large amounts of counterions in the formation

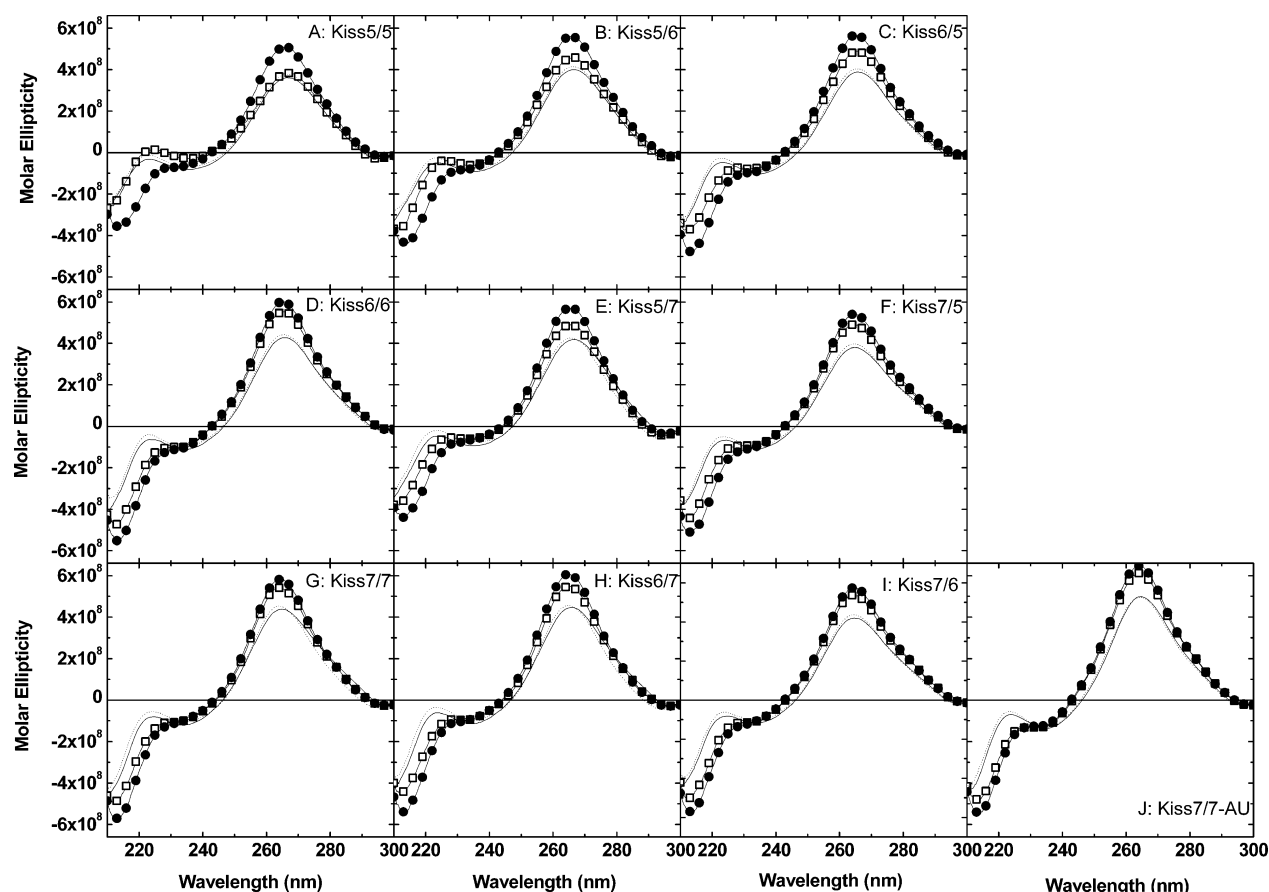


Figure 6. CD spectra of kissing complexes in 850 mM NaCl (open squares) and 0.7 mM MgCl₂ (filled circles) and sum of hairpin components in 850 mM NaCl (thin dotted lines) and 0.7 mM MgCl₂ (thin solid lines). Short complexes: (A) Kiss55, (B) Kiss56, (C) Kiss 65; medium complexes: (D) Kiss 66, (E) Kiss57, (F) Kiss75; long complexes: (G) Kiss77, (H) Kiss67, (I) Kiss76, (J) Kiss77-AU. All experiments were conducted in 10 mM MOPS pH 7, using a total strand concentration of 2.3 μ M (hairpins) or 4.6 μ M (complexes) and normalized as described in the experimental section to represent molar ellipticities.

Table 4. Thermodynamic Profiles for the Formation of Long Na⁺ Kissing Loop Complexes at 25°C^a

complex	T_m °C	ΔH kcal/mol	ΔG kcal/mol	ΔS kcal/mol
850 mM NaCl				
Kiss7/7	33.4° ± 0.1	-60 ± 1	-9.77 ± 0.04	-0.169 ± 0.003
Kiss7/7-AU	39.6° ± 0.4	-61 ± 4	-11.0 ± 0.1	-0.167 ± 0.013
0.7 mM MgCl ₂				
Kiss7/7	57.0° ± 0.1	-47 ± 2	-12.6 ± 0.1	-0.115 ± 0.003
Kiss7/7-AU	61.7° ± 0.5	-43 ± 3	-12.8 ± 0.4	-0.100 ± 0.010

^aAll experiments were conducted in 10 mM MOPS pH 7 and 850 mM NaCl. Thermodynamic profiles correspond to the first transition (kissing loop complex).

of the kissing loop complex. Another important feature of the kissing loop complex is that the apical guanine (the stem guanine closest to the loop, G7 in our hairpins; G7 of R1i is marked with an arrow in Figure 8) is cross-stacked with the guanine in the previous base pair (the one in the second stem base pair, G16 in our hairpins; G16 of R1i is marked with an arrow in Figure 8).⁹ This apical guanine is also making a stacking interaction with the first purine in the loop⁹ (G8 or A8 in our structures). The cross-stack (G7/G16) seems to exist in the individual hairpins,⁹ but the G7/G8 (or G7/A8) stacking

interaction seems to be critical for the kissing loop complex because if the G7-C15 base pair is switched (to C7-G15), the kissing loop complex is significantly destabilized.¹⁸ All these observations suggest that the specific orientation of the bases at the stem–loop junction is critical in the formation of the kissing loop complex and that the formation of the complex builds a significant charge density at the stem–loop interface. Furthermore, the crystal structure of another kissing loop complex shows that the phosphodiester backbone at the stem–loop junction deviates from the A-conformation,²⁸ suggesting again that this region has a unique conformation in loop–loop complexes.

Na⁺ vs Mg²⁺ Kissing Loop complexes. The structure of the ColE1 kissing loop complex⁹ was solved in the presence of 2 mM MgCl₂, and hence it represents the Mg²⁺ kissing loop complex. The Mg²⁺ loop–loop complexes are stable for all stem sizes, suggesting that Mg²⁺ is effective at reducing the electrostatic repulsion arising from the close positioning of bridging phosphates. On the other hand, the majority of the Na⁺ loop–loop complexes are only marginally stable at room temperature, as shown by their relatively low T_m 's. This explains the large Na⁺ concentration required in the titration experiments described above; at lower Na⁺ concentrations the T_m 's of these complexes are probably too low to allow their formation at room temperature. This is consistent with the results reported by Weixlbaumer et al.,²⁶ which show that the DIS type

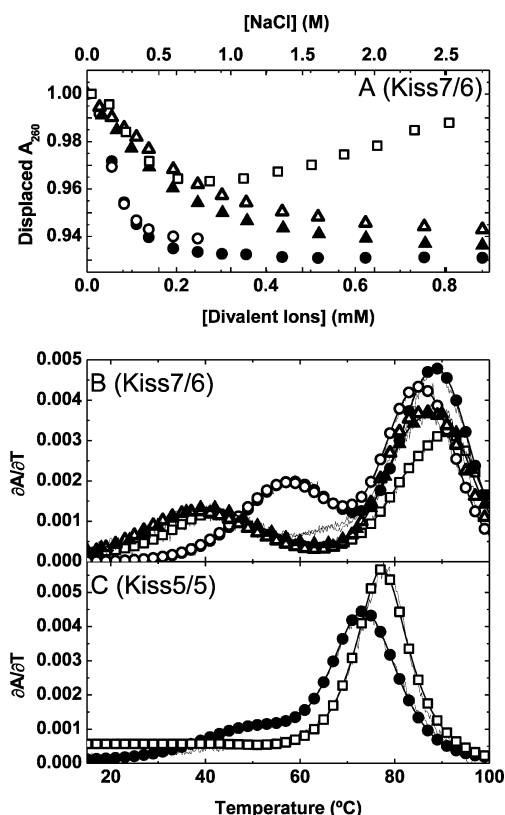


Figure 7. Experiments at various ionic conditions. (A) UV titrations of Kiss7/6 with MgCl₂ (filled circles), CaCl₂ (open circles), SrCl₂ (open triangles), BaCl₂ (filled triangles), NaCl (open squares). All experiments were conducted in 10 mM MOPS pH 7, using a total strand concentration of 7 μ M. (B) Unfolding of Kiss7/6 in 0.88 mM MgCl₂ (filled circles); 0.88 mM CaCl₂ (open circles); 0.88 mM SrCl₂ (open triangles); 0.88 mM BaCl₂ (filled triangles); and 2500 mM NaCl (open squares). All experiments were conducted in 10 mM MOPS pH 7, using a total strand concentration of 3.5 μ M (divalent ions) or 3.1 μ M (NaCl). (C) Unfolding of Kiss5/5 in 0.7 mM MgCl₂ (filled circles) and 2700 mM NaCl (open squares). All experiments were conducted in 10 mM MOPS pH 7, using total strand concentrations of 2.8 μ M. The traces shown in (B) and (C) represent the first derivative of the absorbance vs temperature profiles collected at 260 nm.

kissing loop complex requires more sodium than magnesium ions to reach comparable stabilities. Furthermore, our results suggest that there are differences between the Na⁺ and Mg²⁺ complexes: the Na⁺ complexes show lower decreases in absorbance compared to the Mg²⁺ complexes, there are slight differences in the CD spectra, and the Na⁺ complexes have somewhat larger unfolding enthalpies (55–65 kcal/mol) than the Mg²⁺ complexes (36–48 kcal/mol). We propose that Na⁺ promotes the formation of a kissing loop complex with a looser structure at the stem–loop interface. This idea is supported by molecular dynamics simulations of related kissing loop complexes, which have suggested that in the absence of Mg²⁺, complexes exhibit wider ion pockets and increased fluctuations.³⁰ A looser structure at the stem–loop junction may affect the conformation and stability in the neighboring helical regions (the stem and the loop–loop helices). It follows that slightly decreasing the constraints at the stem–loop interface should facilitate the formation of the kissing loop complex in the presence of NaCl. This is exactly what is observed in the AU-kiss, where we replaced the second stem base pair (C8–G16) with an AU base pair (U8–A16). This complex is more

Table 5. Unfolding Profiles of Kiss7/6 and Kiss5/5 at Various Ionic Conditions^a

[cation]	Transition 1		Transition 2		Transition 3	
	ΔH_1^* kcal/mol	T_{m1} °C	ΔH_2^* kcal/mol	T_{m2} °C	ΔH_3^* kcal/mol	T_{m3} °C
Kiss7/6						
0.88 mM MgCl ₂ ^a	46	58.6	65	85.2	70	91.9
0.88 mM CaCl ₂ ^a	46	57.9	65	82.4	70	89.4
0.88 mM SrCl ₂ ^a	35	39	65	82	70	91
0.88 mM BaCl ₂ ^a	41	41	65	82.5	70	91.5
2500 mM NaCl ^b	49	42	57	84	71	93
Kiss5/5						
0.7 mM MgCl ₂ ^c	39	51	53	73.8	N/A	N/A
2700 mM NaCl ^c	130	77.5	48	77.5	N/A	N/A

^aAll experiments were conducted in 10 mM MOPS pH 7, using total strand concentrations of (a) 3.5 μ M; (b) 3.1 μ M; (c) 2.8 μ M. Please note that the first transition of Kiss5/5 in 0.7 mM MgCl₂ is slightly different from that in Table 2 due to the difference in total strand concentration, which affects the stability of bimolecular transitions.

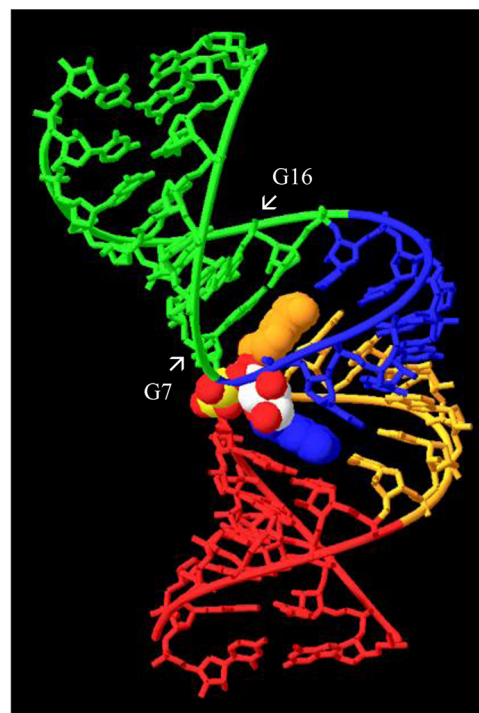


Figure 8. ColE1 kissing loop complex (PDB file 2BJ2⁹). The R1i helix and loop are shown in green and blue, the R2i helix and loop are red and gold. Narrowing of the major groove shortens the distance that the bridging phosphates (spaced filled yellow spheres) cross. The first purines in the loops are shown as spaced filled bases (G8 in R1i is blue and A8 in R2i is gold). The apical guanine of R1i (G7) is cross-stacked with G16 of R1i and also makes stacking interactions with A8 of R2i (gold). Similar stacking interactions occur at the stem-loop interface of R2i. This figure was prepared using the program Swiss-PdbViewer [http://www.expasy.org/spdbv/].²⁹

stable than its GC counterpart, Kiss7/7 (as shown by its larger T_m). These results suggest that decreasing the stability of the

base pairs surrounding the loop-helix junction facilitates the formation of the kissing loop complex, presumably because the less stable AU base pairs have more conformational flexibility than the GC base pairs. A looser structure at the stem-loop junction also explains why the complexes containing five base-pairs in the stem tend to form alternative structures. The remaining ~ 3 base pairs are not able to maintain the structure of the hairpin and the formation of an extended duplex is favored.

AU Base Pairs at the Stem-Loop Interface. The fact that the AU-Kiss complex forms more effectively than the other kissing complexes in the absence of Mg^{2+} may be explained in two ways. First, the lower stability of the AU base pair (U6-A16) and base pair stack may allow more conformational flexibility around the stem-loop interface. Since this base pair is immediately before the apical guanine (G7), the increased conformational flexibility of U6-A16 may allow the apical base pair (G7-C15) to move more freely into its position in the kissing loop complex while allowing the phosphates around the stem-loop interface (for example U6-A16) to be further apart. Second, it is also possible that the substitution of G16 for A16 removes a ligand from a Mg^{2+} binding site (presumably the O6 of G16). This is supported by Mn^{2+} binding experiments,⁹ which reveal a metal binding site near G16 of R2i. It is interesting to note that another set of kissing loop complexes displays a similar relief of the Mg^{2+} requirement resulting from changes in sequence. The dimerization initiation site (DIS) from HIV-1 is a loop-loop complex in which minor variations in the sequence result in two different types of complex: Lai and Mal.⁶ These complexes differ in only four bases (three in the loop and one in the second base pair of the stem, equivalent to our C6-G16 position). However, the Mal complex requires Mg^{2+} while the Lai complex can form in the absence of Mg^{2+} .^{6,14} Although the authors attribute the difference to a Mg^{2+} binding site on the O6 of a guanine in the Mal loop (which is replaced by a uridine in Lai), it is interesting to note that the Lai sequence has a weaker base pair in the second position of the stem (Lai has a GU base pair while Mal has an AU base pair). It is possible that this weaker base pair also contributes to removing the Mg^{2+} requirement of this kissing loop complex.

Specific Ion Sites. The fact that Mg^{2+} is more effective than Na^+ at forming kissing loop complexes may be due to the electrostatic advantage of having two positive charges or to the presence of specific Mg^{2+} sites in the complex. The NMR structure of the complex⁷ describes phosphate clusters (formed by the phosphates in bases G7, A9 and C/U10 in each hairpin) that could represent Mg^{2+} binding sites, but the authors point out that Mn^{2+} experiments do not implicate these regions as specific metal ion sites. Divalent cations are generally much more effective than monovalent cations at stabilizing RNA structures, and it has been suggested that part of the reason for their ability to stabilize RNA is the lower entropic cost associated with accumulating one divalent ion as opposed to two monovalent ions.¹¹ Since Na^+ is a monovalent ion, more ions need to accumulate to stabilize the kissing complexes and as a result, it is much less effective. However, a simple electrostatic advantage does not explain why the larger ions (Sr^{2+} and Ba^{2+}) form less stable complexes than the smaller ions (Mg^{2+} and Ca^{2+}). On the other hand, the fact that Mg^{2+} and Ca^{2+} result in very similar complexes suggests that there are no specifically coordinated Mg^{2+} ions. A similar stabilization by small ions has been observed in the formation of related kissing

loop complexes, and it has been suggested that smaller, higher charge density ions can approach the RNA more closely at regions of high charge density.¹³ We reason that the small ionic radius of Ca^{2+} and Mg^{2+} (0.99 and 0.66 Å, respectively³¹) allows these ions to penetrate into regions of high electrostatic potential, while Sr^{2+} and Ba^{2+} (with ionic radius of 1.12 and 1.34 Å, respectively³¹) may be too big to approach these regions. Although the ionic radius of Na^+ (0.97 Å³¹) is similar to that of Ca^{2+} , the lower charge density of this monovalent ion makes it less effective at stabilizing the kissing loop complexes.

Our overall results suggest that formation of the Na^+ kissing loop complexes requires looser conformations of the base pairs near the loop and that this conformation is easier to attain when less stable AU base pairs are present at the stem-loop interface. We speculate that this facilitation arises from an increased conformational flexibility near the loops, resulting in a lower entropic penalty for the formation of kissing loop complexes containing stems with less stable base pairs near the loop.

Technical Remarks. Researchers interested in following the association of kissing loop complexes in UV titrations should keep in mind that such experiments may have long equilibration times. The UV titrations shown in Figure 2 are conducted by adding increasing amounts of cations to mixtures of the corresponding hairpins. Each point equilibrates very slowly, especially at the lower ion concentrations. The first few points of the titrations take 30–60 min to equilibrate, but the points equilibrate faster as the concentration of ions in solution increases. Kinetic studies have shown that the ColE1 kissing loop complexes form on the second time scale.²⁴ The inverted ColE1 complex (the sequence used in this work) was shown to associate with a rate constant 20 times slower than the original complex, but still in the second time scale ($1 \times 10^5 \text{ M}^{-1} \text{ s}^{-1}$).²⁴ However, those experiments were conducted at higher MgCl_2 concentrations than our experiments (10 mM Mg^{2+} compared to 0.03 mM Mg^{2+} for the first point of our titrations). Faster equilibration times with increasing amounts of ions are expected since these complexes are relatively simple and are therefore likely to have only on-pathway kinetic intermediates,³² if any intermediates are present. The slow equilibration times in our experiments may be explained by the conformational changes that need to occur to form the kissing loop complexes, since the formation of these complexes creates regions of high charge density that are not very stable at low ion concentrations.

CONCLUSION

Our results show that the ColE1 hairpins containing at least six base-pairs in the stem can form kissing loop complexes in the presence of Na^+ or Mg^{2+} . Previous work has shown that the kissing loop complexes formed in the presence of Mg^{2+} contain regions of high charge density at the stem-loop interface.⁹ Our results suggest that the formation of kissing loop complexes requires specific conformations at the stem-loop interface because the kissing loop complexes form more readily when a GC base pair is replaced with a less stable and therefore more conformationally flexible AU base pair. Since Na^+ is less effective than Mg^{2+} at stabilizing regions of high charge density, it is possible that the phosphates in the Na^+ kissing loop complexes may extend further apart resulting in complexes that are more loosely packed at the stem-loop interface. Consistent with this idea, hairpins that are too short to tolerate this suggested loosely packed stem-loop conformation form

extended duplexes rather than kissing loop complexes. The formation of an extended duplex with our short hairpins raises the possibility that the increase in charge density upon formation of a kissing loop complex can be alleviated by changes at the stem-loop interface and subsequent formation of an extended duplex, suggesting a mechanism for the progression from a kissing loop complex to an extended duplex. Our results contribute to a better understanding of the rules governing the formation of kissing loop complexes, which are important to rationalize the principles of RNA-RNA recognition.

AUTHOR INFORMATION

Corresponding Author

*E-mail: asoto@towson.edu; phone: 410-704-2605; fax: 410-704-4265.

Funding

This work was funded in part by a Henry C. Welcome Fellowship (A.M.S.), Towson University Start Up Funds (A.M.S.), Towson University Faculty Development and Research Grant (A.M.S.), Ronald and Linda Raspet Fellowship (G.C.), and Fisher College of Science and Mathematics Undergraduate Research and Travel Grants (G.C. & P.S.).

Notes

The authors declare no competing financial interest.

ACKNOWLEDGMENTS

We thank Dr. David Draper for his crucial input on the initial stages of this work, very helpful suggestions, and for allowing us to use several instruments in his laboratory. We thank Dr. Donald Rau for helpful discussions of this work, Dr. Stephen Scales for proofreading our manuscript, Mr. George Kram and Ms. Leetta Abner for their assistance with the various supplies needed throughout this work, and the two anonymous reviewers of this manuscript for their helpful comments and suggestions.

ABBREVIATIONS AND TEXTUAL FOOTNOTES

MOPS: 3-morpholinopropanesulfonic acid; Kiss5/5, Kiss6/6, Kiss5/7, Kiss7/5, Kiss7/7, Kiss 6/7, Kiss7/6, Kiss7/7-AU: Designation for the molecules used in this study; DIS: dimerization initiation signal; CD: circular dichroism; ΔS_{fold} : entropy of folding; ΔH_{fold} : enthalpy of folding

REFERENCES

- (1) Cooper, T. A., Wan, L., and Dreyfuss, G. (2009) RNA and disease. *Cell* 136, 777–793.
- (2) Altuvia, S., and Wagner, E. G. (2000) Switching on and off with RNA. *Proc. Natl. Acad. Sci. U. S. A.* 97, 9824–9826.
- (3) Batey, R. T., Rambo, R. P., and Doudna, J. A. (1999) Tertiary Motifs in RNA Structure and Folding. *Angew. Chem., Int. Ed. Engl.* 38, 2326–2343.
- (4) Brunel, C., Marquet, R., Romby, P., and Ehresmann, C. (2002) RNA loop-loop interactions as dynamic functional motifs. *Biochimie* 84, 925–944.
- (5) Chen, A. A., Draper, D. E., and Pappu, R. V. (2009) Molecular simulation studies of monovalent counterion-mediated interactions in a model RNA kissing loop. *J. Mol. Biol.* 390, 805–819.
- (6) Ennifar, E., Walter, P., Ehresmann, B., Ehresmann, C., and Dumas, P. (2001) Crystal structures of coaxially stacked kissing complexes of the HIV-1 RNA dimerization initiation site. *Nat. Struct. Biol.* 8, 1064–1068.
- (7) Tan, Z. J., and Chen, S. J. (2010) Predicting ion binding properties for RNA tertiary structures. *Biophys. J.* 99, 1565–1576.

- (8) Chang, K. Y., and Tinoco, I., Jr. (1997) The structure of an RNA "kissing" hairpin complex of the HIV TAR hairpin loop and its complement. *J. Mol. Biol.* 269, 52–66.
- (9) Lee, A. J., and Crothers, D. M. (1998) The solution structure of an RNA loop-loop complex: the ColE1 inverted loop sequence. *Structure* 6, 993–1005.
- (10) Draper, D. E., Grilley, D., and Soto, A. M. (2005) Ions and RNA folding. *Annu. Rev. Biophys. Biomol. Struct.* 34, 221–243.
- (11) Draper, D. E. (2004) A guide to ions and RNA structure. *RNA* 10, 335–343.
- (12) Singh, A., Sethaphong, L., and Yingling, Y. G. (2011) Interactions of cations with RNA loop-loop complexes. *Biophys. J.* 101, 727–735.
- (13) Lambert, D., Leipply, D., Shiman, R., and Draper, D. E. (2009) The influence of monovalent cation size on the stability of RNA tertiary structures. *J. Mol. Biol.* 390, 791–804.
- (14) Lodmell, J. S., Paillart, J. C., Mignot, D., Ehresmann, B., Ehresmann, C., and Marquet, R. (1998) Oligonucleotide-mediated inhibition of genomic RNA dimerization of HIV-1 strains MAL and LAI: a comparative analysis. *Antisense Nucleic Acid Drug Dev.* 8, 517–529.
- (15) Jossinet, F., Paillart, J. C., Westhof, E., Hermann, T., Skripkin, E., Lodmell, J. S., Ehresmann, C., Ehresmann, B., and Marquet, R. (1999) Dimerization of HIV-1 genomic RNA of subtypes A and B: RNA loop structure and magnesium binding. *RNA* 5, 1222–1234.
- (16) Owczarzy, R. "Extinction (absorption) coefficients of nucleic acids calculated at 260 nm" 2012. <<http://www.owczarzy.net/extinct.htm>> (accessed 21 March, 2012).
- (17) Grilley, D., Soto, A. M., and Draper, D. E. (2009) Direct quantitation of Mg²⁺-RNA interactions by use of a fluorescent dye. *Methods Enzymol.* 455, 71–94.
- (18) Gregorian, R. S., Jr., and Crothers, D. M. (1995) Determinants of RNA hairpin loop-loop complex stability. *J. Mol. Biol.* 248, 968–984.
- (19) Marky, L. A., and Breslauer, K. J. (1987) Calculating thermodynamic data for transitions of any molecularity from equilibrium melting curves. *Biopolymers* 26, 1601–1620.
- (20) Draper, D. E., and Gluick, T. C. (1995) Melting studies of RNA unfolding and RNA-ligand interactions. *Methods Enzymol.* 259, 281–305.
- (21) Draper, D. E., Bukhman, Y. V., and Gluick, T. C. (2001) Thermal methods for the analysis of RNA folding pathways. *Curr. Protoc. Nucleic Acid Chem.*, Chapter 11, Unit 11.3.
- (22) Tinoco, I., Sauer, K., Wang, J. C., Puglisi, J. D. (2001) *Physical Chemistry: Principles and Applications in Biological Sciences*, 4th ed., p 574, Prentice Hall, Upper Saddle River, NJ.
- (23) Kelly, S. M., Jess, T. J., and Price, N. C. (2005) How to study proteins by circular dichroism. *Biochim. Biophys. Acta* 1751, 119–139.
- (24) Eguchi, Y., and Tomizawa, J. (1991) Complexes formed by complementary RNA stem-loops. Their formations, structures and interaction with ColE1 Rom protein. *J. Mol. Biol.* 220, 831–842.
- (25) Xia, T., SantaLucia, J., Jr., Burkard, M. E., Kierzek, R., Schroeder, S. J., Jiao, X., Cox, C., and Turner, D. H. (1998) Thermodynamic parameters for an expanded nearest-neighbor model for formation of RNA duplexes with Watson-Crick base pairs. *Biochemistry* 37, 14719–14735.
- (26) Weixlbaumer, A., Werner, A., Flamm, C., Westhof, E., and Schroeder, R. (2004) Determination of thermodynamic parameters for HIV DIS type loop-loop kissing complexes. *Nucleic Acids Res.* 32, 5126–5133.
- (27) Shikhiya, R., Li, J. S., Gold, B., and Marky, L. A. (2005) Incorporation of cationic chains in the Dickerson-Drew dodecamer: correlation of energetics, structure, and ion and water binding. *Biochemistry* 44, 12582–12588.
- (28) Lebars, I., Legrand, P., Aimé, A., Pinaud, N., Fribourg, S., and Di Primo, C. (2008) Exploring TAR-RNA aptamer loop-loop interaction by X-ray crystallography, UV spectroscopy and surface plasmon resonance. *Nucleic Acids Res.* 36, 7146–7156.

- (29) Guex, N., and Peitsch, M. C. (1997) SWISS-MODEL and the Swiss-PdbViewer: an environment for comparative protein modeling. *Electrophoresis* 18, 2714–2723, <http://www.expasy.org/spdbv/>.
- (30) Réblová, K., Spacková, N., Sponer, J. E., Koca, J., and Sponer, J. (2003) Molecular dynamics simulations of RNA kissing-loop motifs reveal structural dynamics and formation of cation-binding pockets. *Nucleic Acids Res.* 31, 6942–6952.
- (31) Weast, R. C., Ed (1964) *CRC Handbook of Chemistry and Physics*, 49th ed., p F152, The Chemical Rubber Company, Cleveland, OH
- (32) Mitra, S. Brenowitz, M. (2009) Metal Ions and RNA Folding in *Nucleic Acid – Metal Ion Interactions* (Hud, N. V., Ed) pp 221–259, Royal Society of Chemistry, Cambridge.